NASA TECHNICAL MEMORANDUM

NASA TM X-68043

NASA TM X-68043

CASE FILE COPY

PROCEDURE FOR ESTIMATING EFFECTS OF ION BEAM INTERACTION WITH SPACECRAFT

by Thaine W. Reynolds
Lewis Research Center
Cleveland, Ohio
April, 1972

This information is being published in preliminary form in order to expedite its early release.

ABSTRACT

Procedure for calculating various interactions of neutral and charged particle efflux from ion thrusters with spacecraft surfaces is outlined. Calculation details are referenced. Details of charge-exchange calculation in the near-field of the thruster are presented.

E-6880

PROCEDURE FOR ESTIMATING EFFECTS OF ION BEAM INTERACTION WITH SPACECRAFT

by Thaine W. Reynolds

Lewis Research Center

E-6880

SUMMARY

Each spacecraft layout involving electrostatic thrusters presents its own unique set of conditions which should be systematically checked for possible interaction between the ion beam and spacecraft components. For this reason, this report presents an outline of the procedure that has been followed by the author at the Lewis Research Center to check possible spacecraft contamination from ion thruster operation.

Details of calculation procedure are not presented if they are available in already published references. The references are cited in each instance.

Details and graphical results of charge exchange calculations are presented since this material has not been previously published.

INTRODUCTION

The possible problems associated with the effects of the thruster exhaust on various spacecraft components for spacecraft employing electrostatic thrusters have been enumerated and discussed in previous publications (refs. 1 to 8). Since each spacecraft design or layout is unique, it is necessary to follow through some general procedure to check all interaction possibilities to be assured that no detrimental effects will be encountered.

The purpose of this report is to summarize a general procedure that has been followed at Lewis Research Center. It includes all the interaction effects associated with particle efflux from the thrusters

that have been considered as possibly detrimental. Calculation details are not presented if they are available in already published references. The appropriate references are cited.

A procedure used in calculation of charge-exchange neutral and ion formation rates is discussed in some detail, since the method used has not been published previously.

ANALYTICAL PROCEDURE

The following sketch illustrates the principal types and sources of particle efflux from ion thrusters that are of sufficient magnitude to affect possible spacecraft components and are considered in the analysis.

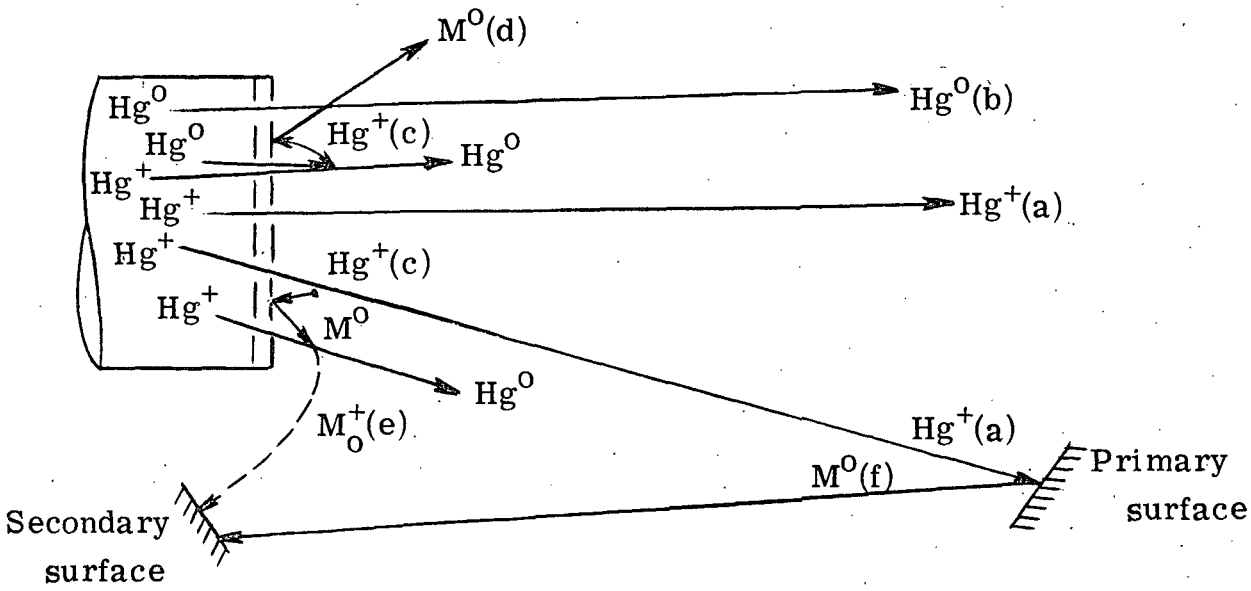

Sketch a

Types of particle flux illustrated are:

(a) Main beam propellant ions (fast Hg^+)

(b) Propellant neutrals resulting from beam inefficiency (slow Hg^O)

(c) Propellant ions from charge exchange between (a) and (b) (slow Hg^+)

(d) Grid metal neutrals sputtered by (c) ions (slow M^o)

(e) Grid metal ions from charge exchange between (a)-ions and (d)-neutrals (slow M^+)

(f) Neutral atoms sputtered from a primary surface by (a)-ions (slow M^o)

The problems associated with these fluxes may arise from sputtering caused by the impingement of the higher energy particles, or from build-up of a layer of condensate of the arriving material.

Items (a), (b), and (d) are of concern only with surfaces in line-of-sight with the thruster exit plane (referred to as primary surfaces). Items (c), (e), and (f) may be concerned as well with surfaces which are not in line-of-sight of the thruster exit plane (referred to as secondary surfaces).

Information Required

The following items of information are required:

(1) Design layout of the spacecraft, including ion engine and all components that might be affected by sputtering or condensation of material.

(2) Thruster data

(a) Size (radius R_o)

(b) Operating data: total propellant flow, propellant utilization efficiency, accelerator impingement current, accel-decel voltages

(c) Experimental ion-beam profile at operating conditions, taken sufficiently far downstream to be representative of the far-field profile (i.e., at $Z/R_o \geq 8$)

PROCEDURE

The following list constitutes essentially the procedure followed. The references cited in each item contain the detailed discussions of that particular phase of the calculations.

(1) The far-field experimental ion beam profile data is fitted by the equation

$$\frac{j(\theta)}{j(0)} = e^{-[\lambda(1-\cos\theta)]^n} \qquad (1)$$

to determine the constants n and λ (ref. 9). This equation, with the determined values of n and λ, is then used in all subsequent calculations requiring use of an ion beam density value at any location beyond an axial distance, $Z/R_0 \geq 8$. Calculations requiring values of ion beam density at locations closer than $Z/R_0 = 8$ are treated differently as will be noted later.

(2) Using equation (1), constant current density lines are plotted on the spacecraft layout (or on a transparent overlay to scale) to check ion-impingement current values on any primary surface. (Plots are illustrated by fig. 9 of ref. 9.)

(3) The ion impingement currents, determined in item (2), and a knowledge of the sputtering coefficient (refs. 10 and 11) are combined to determine the sputtering rate for any primary surface.

(4) View factors (refs. 6, 12, and 13) from primary surfaces to any sensitive secondary surface are determined. The product of these view factors and the sputtering rate determined in item (3) are checked to see if the arrival rate of sputtered material from the primary surface is of sufficient magnitude to cause any problem (ref. 7).

(5) View factors (refs. as item 4) from the thruster to any primary surface are determined. (A plot of constant view factor lines similar to that made for ion current density mentioned in item 2 is a convenient way of exhibiting these.) These view factors are applied to neutral

emission rates of both neutral propellant atoms and sputtered grid neutrals. The corresponding arrival rates are compared with desorption rates at the surface temperatures to see if condensing conditions exist (ref. 6). If so, determine whether the condensation rates are high enough to cause a problem over the mission duration (refs. 2, 7, and 8).

(6) If the neutral arrival rates calculated in item (5) are not high enough to condense on primary surfaces, their subsequent arrival rates on any secondary surface are checked (ref. 7).

(7) Charge-exchange formation rates are calculated for both propellant atoms and sputtered grid metal atoms. The procedure and some graphical results are presented in the CHARGE EXCHANGE section of this report.

The subsequent trajectories of these charge exchange ions is a matter of conjecture at this time. Since these ions are principally low velocity they are expected to follow whatever electric field lines exist in their vicinity. Several types of assumption have been made as to their trajectories, including: (a) that the charge exchange ions travel radially outward (i.e., radially from the ion beam centerline) from the point of their formation, (b) that they travel normal to some defined "beam-spreading" angle, and (c) that they disperse spherically symmetrically from the point of their formation, essentially as if no general electric field existed to guide them elsewhere. Experimental data in this area is needed to better define this problem.

CHARGE EXCHANGE

This section gives the details of the charge exchange calculation for ion thrusters.

A major portion of the total charge exchange reactions takes place within a few thruster radii of the thruster exit. The use of the simplified far-field relations for current density and neutral density are thus not justified in this calculation. In the following development applicable near-field relations are used.

The following sketch shows the definitions of variables used.

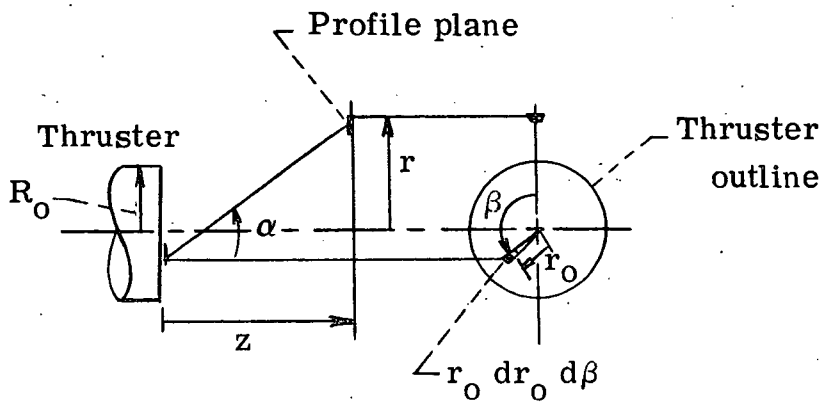

The total number of ions exchanging charge in an elemental volume at (r, z) is

$$dN = \sigma_{10} \mu_i n_o \, dV = \sigma_{10} \mu_i n_o \, dS \, dZ \tag{2}$$

(Symbols are defined in the appendix.) In the cylindrically symmetric case, using ring elements, $dS = 2\pi r \, dr$.

In this development, a specific distribution for the ion emission rate across the emitter face is assumed, namely,

$$\frac{j(r_o, o)}{j(o, o)} = \cos\left(\frac{\pi}{2} \frac{r_o}{R_o}\right) \tag{3}$$

The ion arrival rate at the point (r, z) is accordingly given by the following expression (developed in appendix B of ref. 9)

$$\mu_i = \bar{\nu} \frac{2.16 \, C(n, \lambda)}{\pi z^2} \mathcal{J}(r_o, \beta) \tag{4}$$

where

$$\mathcal{J}(r_o, \beta) = \int_{A_o} \cos\left(\frac{\pi}{2}\frac{r_o}{R_o}\right) \exp\left[-\lambda\left(1 - \frac{z}{\sqrt{r_o^2 + r^2 - 2rr_o\cos\beta + z^2}}\right)\right]^n r_o\, dr_o\, d\beta \qquad (5)$$

The neutral atom density, n_o, at the point (r, z) is calculated from the neutral arrival rate by,

$$n_o(r, z) = \frac{\mu_o(r, z)}{v_o} \qquad (6)$$

This relation assumes all trajectories are parallel. It will yield slightly lower neutral density estimates close to the thruster where the applicable relation for $\mu_o \cong \frac{1}{2} n_o v_o$; v_o is the thermal velocity, $\sqrt{8kT/\pi m}$.

The neutral atom arrival rate is determined by the relation

$$\mu_o(r, z) = C_1 \bar{\nu} F_{12}[1 - f(x)] \qquad (7)$$

where

C_1 fraction of average ion emission rate that represents neutral emission rate

$\bar{\nu}$ average ion emission rate, $I_a/q\pi R_o^2$

F_{12} view factor from thruster to point (r, z)

$f(x)$ fraction of total neutrals emitted which have undergone charge exchange up to axial station, x

The view factor F_{12} for a disk source, assuming uniform neutral emission rate across the surface is, (ref. 13)

$$F_{12} = \frac{1}{2}\left[1 - \frac{1 + y^2 - \frac{1}{x^2}}{\sqrt{\left(1 + y^2 + \frac{1}{x^2}\right)^2 - 4\frac{y^2}{x^2}}}\right] \tag{8}$$

where $x = Z/R_o$, and $y = r/z$.

Substituting (4), (6), and (7) into (2) and indicating integration over all variables (r_o from o to R_o; β from o to 2π; r from o to ∞; z from o to z) yield

$$\dot{N} = \sigma_{10}\int\left[\bar{\nu}\frac{2.16\,C(n,\lambda)}{\pi z^2}\,\mathcal{Q}(r_o,\beta)\right]\left[C_1\bar{\nu}F_{12}(1 - f(x))\sqrt{\frac{\pi m}{8kT}}\right]2\pi r\,dr\,dz \tag{9}$$

But, the fraction of total neutrals emitted which have reacted up to distance x is

$$f(x) = \frac{\dot{N}(x)}{\pi R_o^2 C_1 \bar{\nu}} \tag{10}$$

Combining (10) and (9) and converting to dimensionless variables yield

$$f(x) = \frac{A}{2}\int_{x=o}^{x}\left[\int_{y=o}^{\infty} I(w,\beta)\left[F_{12}(1 - f(x))\right] y\,dy\,dx\right] \tag{11}$$

where

$$A = \frac{8.64\ \sigma_{10} C(n,\lambda)\bar{\nu} R_o}{\pi\sqrt{\frac{8kT}{\pi m}}}$$

$$I(w,\beta) = \frac{\mathcal{Q}(r_o,\beta)}{R_o^2} \qquad (12)$$

$$w = \frac{r_o}{R_o}$$

Equation (11) was solved numerically for various values of A. Since A (eq. (12)) contains several variables it was evaluated for one set of conditions. It can then be expressed in terms of ratios to these "standard" values.

The following values might be typical of a 30-centimeter diameter thruster using mercury propellant:

$n = 1$	$R_o = 15$ cm	$T = 500$ K	$C(n,\lambda) = 10.92$
$\lambda = 25$	$I_a = 1.5$ a	$m = 200$ (Hg)	$\sigma_{10} = 6\times10^{-15}$ cm^2

The resulting value of A for these conditions is 1.56. Thus,

$$A = 1.56\left(\frac{\sigma_{10}}{6\times10^{-15}}\right)\left(\frac{C(n,\lambda)}{10.92}\right)\left(\frac{j_a/cm^2}{0.00212}\right)\left(\frac{500}{T}\right)^{1/2}\left(\frac{m}{200}\right)^{1/2}\left(\frac{R_o}{15}\right) \qquad (13)$$

Charge-exchange cross-section values are available for some of the reactions of interest (refs. 14 to 17), but have only been estimated for others of primary concern (ref. 18).

A plot of the fraction of emitted neutrals which have engaged in charge exchange as a function of the distance from the thruster is shown in figure 1. The corresponding charge exchange formation rate at any location is shown in figure 2. In these plots several A-values are shown. A change in A-value can represent a change in any one or several of the parameters indicated in equation (13). Several λ-values are also shown, representing the range from a fairly collimated beam ($n = 1$, $\lambda = 60$) to one more divergent ($n = 1$, $\lambda = 25$). A caution in interpretation is to be noted here. While it appears that a less well collimated beam has more charge exchange than a more directed beam (comparing, say curves for $A = 1$ for the ($n = 1$, $\lambda = 25$) and ($n = 1$, $\lambda = 60$) conditions) it should be remembered that A contains the parameter $C(n, \lambda)$. The same value of A for these two cases, then, does not represent otherwise identical conditions. When this is taken into account, it will be found that there is little difference in charge exchange formation in comparing just the effect of beam divergence. Values of $C(n, \lambda)$ may be found in reference 9.

Some other points that may be noted in figures 1 and 2 are:

(1) Most of the charge-exchange interaction that occurs will have taken place by about 8 to 10 thruster radii downstream.

(2) Beyond about 8 thruster radii, the charge exchange formation rate varies inversely with the square of the distance (fig. 2).

(3) Below about 10 percent reacted, the charge-exchange formation is proportional to A. Fraction reacted at some value of A not plotted is thus readily estimated

$$f(x) = [f(x)]_{ref} \cdot \frac{A}{A_{ref}}$$

CONCLUDING REMARKS

Each spacecraft layout involving electrostatic thrusters presents its own unique set of conditions which should be systematically checked for possible interaction between the ion beam and spacecraft components. For this reason, this report has presented an outline of the procedure that has been followed by the author at the Lewis Research Center to check the possible spacecraft contamination from ion thruster operation.

Details of the calculation procedure have not been presented if they were available in already published references. The references have been cited in each instance.

Details and graphical results of charge-exchange calculations were presented since this particular material has not been published previously.

APPENDIX - SYMBOLS

A	constant, defined by eq. (12)
$C(n,\lambda)$	constant in ion profile equation
C_1	fraction of average ion emission rate that represents neutral emission rate
F_{12}	view (or configuration) factor
f	fraction of emitted neutrals that have exchanged charge
I_a	total current, a
$I(w,\beta)$	integral in eq. (11)
$\mathcal{J}(r_o,\beta)$	integral in eq. (4), defined in eq. (5)
$j(o)$	current density on center line, $\theta = o$
$j(\theta)$	current density in radial plane at angle θ from beam centerline
k	Boltzmann constant
m	particle mass
$\dot{N}$	total number of ions exchanging charge
n	constant in ion flux eq. (1)
n_o	neutral particle density
q	electron charge
R_o	radius of thruster
r	radial distance in plane downstream of thruster
r_o	radial distance in thruster exit plane
S	area
T	temperature, K
V	volume

v_o particle velocity

w dimensionless radial variable $\equiv (r_o/R_o)$

x dimensionless length variable $\equiv Z/R_o$

y dimensionless radial variable $\equiv r/Z$

Z axial distance from thruster exit

α angle variable (sketch (a))

β angle variable in thruster exit plane (sketch (a))

θ angle between thruster centerline and trajectory leaving thruster exit center

λ constant in ion beam profile eq. (1)

μ_i ion arrival rate per unit area

$\overline{\nu}$ average ion emission rate from thruster $\equiv I_a/q\pi R_o^2$

REFERENCES

1. Kerslake, William R.: Charge-Exchange Effects on the Accelerator Impingement of an Electron-Bombardment Ion Rocket. NASA TN D-1657, 1963.

2. Staggs, John F.; Gula, William P.; and Kerslake, William R.: Distribution of Neutral Atoms and Charge-Exchange Ions Downstream of an Ion Thruster. J. Spacecraft Rockets, vol. 5, no. 2, Feb. 1968, pp. 159-164.

3. Kerslake, William R.; Byers, David C.; and Staggs, John F.: SERT II-Mission and Experiments. J. Spacecraft Rockets, vol. 7, no. 1, Jan. 1970, pp. 4-6.

4. Hall, David F.; Newman, Brian E.; and Womack, James R.: Electrostatic Rocket Exhaust Effects on Solar-Electric Spacecraft Subsystems. J. Spacecraft Rockets, vol. 7, no. 3, Mar. 1970, pp. 305-312.

5. Anon.: A Study of Cesium Exhaust From an Ion Engine and Its Effects Upon Several Spacecraft Components. Rep. HIT-399, Hittman Assoc., Inc., June 26, 1969.

6. Reynolds, Thaine W.; and Richley, Edward A.: Distribution of Neutral Propellant From Electric Thrusters Onto Spacecraft Components. NASA TN D-5576, 1969.

7. Reynolds, Thaine W.; and Richley, Edward A.: Contamination of Spacecraft Surfaces Downstream of a Kaufman Thruster. NASA TN D-7038, 1971.

8. Staskus, John V.; and Burns, Robert J.: Deposition of Ion Thruster Effluents on SERT II Spacecraft Surfaces. Paper 70-1128, AIAA, Aug. 1970.

9. Reynolds, Thaine W.: Mathematical Representation of Current Density Profiles From Ion Thrusters. NASA TN D-6334, 1971.

10. Wehner, G. K.; and Rosenberg, D.: Mercury Ion Beam Sputtering of Metals at Energies 4-15 kev. J. Appl. Phys., vol. 32, no. 5, May 1961, pp. 887-890.

11. Carter, G.; and Colligon, J. S.: Ion Bombardment of Solids. American Elsevier Publ. Co., Inc., 1968.

12. Howell, John R.; and Siegel, Robert: Thermal Radiation Heat Transfer. Vol. 2: Radiation Exchange Between Surfaces and in Exclosures. NASA SP-164, Vol. II, 1969, pp. 241-275.

13. Reynolds, Thaine W.; and Richley, Edward A.: Free-Molecule Flow and Surface Diffusion Through Slots and Tubes - A Summary. NASA TR R-255, 1967.

14. McDaniel, Earl W.: Collision Phenomena in Ionized Gases. John Wiley & Sons, Inc., 1964.

15. von Engel, A.: Ionized Gases. Second ed., Clarendon Press, Oxford, 1965.

16. Marino, Lawrence L.; Smith, A. C. H.; and Caplinger, E.: Charge Transfer Between Position Cesium Ions and Cesium Atoms. Phys. Rev., vol. 128, no. 5, Dec. 1, 1962, pp. 2243-2250.

17. Zuccaro, D. E.: Measurement of the Resonant Charge-Exchange Cross Section of Mercury and Cesium. Paper 67-682, AIAA, Sept. 1967.

18. Dugan, John V., Jr.: Upper-Limit Charge Exchange Cross Sections for Mercury$^+$ on Molybdenum and Cesium$^+$ on Aluminum. NASA TM X-2527, 1972.

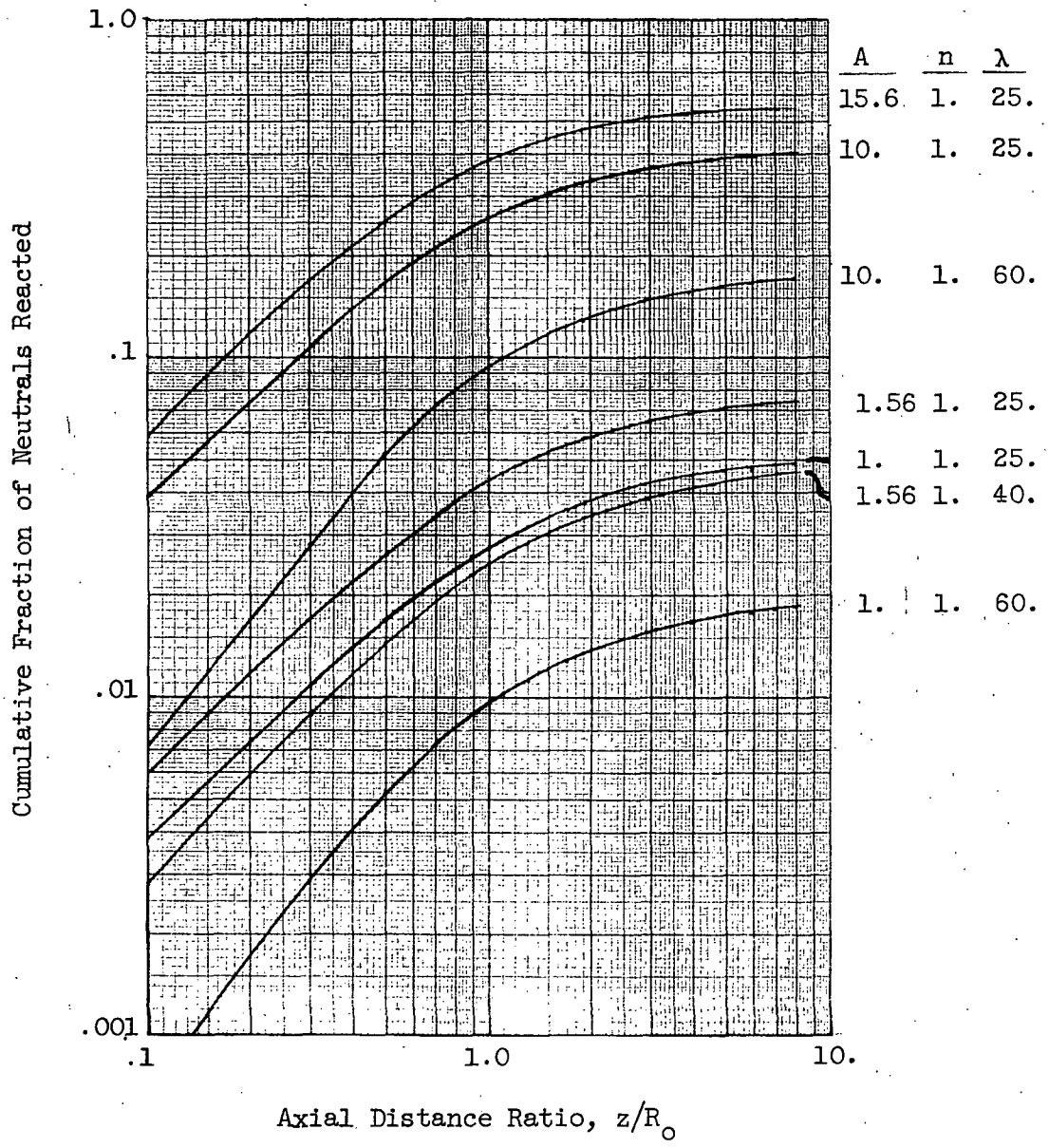

Figure 1. - Variation of charge exchange neutral fraction with distance from thruster exit. (n, λ) determined by equation (1); A by equation (13).

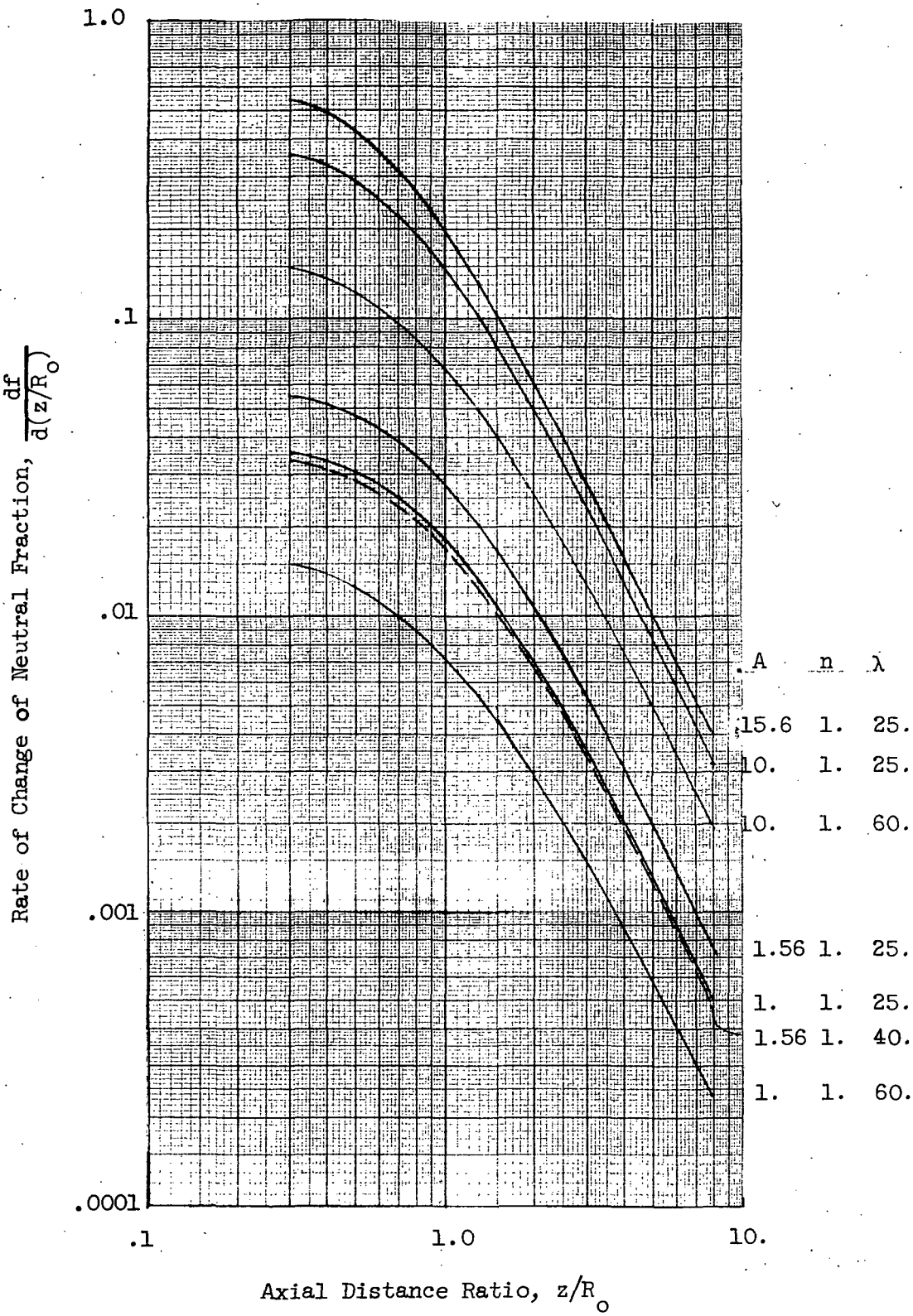

Figure 2. - Variation of charge-exchange formation rate with distance from thruster exit. (n, λ) determined by equation (1); A by equation (13).

NASA-Lewis-Com'l